PERMANENT DEACTIVATION OF THE BORON-OXYGEN RECOMBINATION CENTER IN SILICON SOLAR CELLS

Bianca Lim, Sonja Hermann, Karsten Bothe, Jan Schmidt, and Rolf Brendel
Institut für Solarenergieforschung Hameln (ISFH)
Am Ohrberg 1, D-31860 Emmerthal, Germany

ABSTRACT: The permanent deactivation of the recombination-active boron-oxygen complex, which consists of one substitutional boron atom and one interstitial oxygen dimer, in boron-doped Czochralski-grown silicon is demonstrated on low-resistivity lifetime samples as well as on high-efficiency RISE-EWT (Rear Interdigitated Single Evaporation Emitter Wrap-Through) solar cells. Furthermore, we describe a model capable of explaining the time dependence of the lifetime evolution during the deactivation process, introducing a second defect reaction which results in the binding of the oxygen dimer in a recombination-inactive complex. The application of the deactivation procedure to RISE-EWT solar cells results in an increase of the stabilized energy conversion efficiency from 19.1 % to 20.3 %.

Keywords: Czochralski, Defects, High-Efficiency, Modelling

1 INTRODUCTION

The energy conversion efficiency of solar cells made on oxygen-rich boron-doped silicon, such as B-doped Czochralski silicon (Cz-Si), is limited by a recombination-active boron-oxygen complex [1], which forms under illumination via a recombination-enhanced defect reaction and consists of one substitutional boron atom (B_s) and one interstitial oxygen dimer (O_{2i}) [2]. Since the B_sO_{2i} complex dissociates at higher temperatures (> 170 °C), the degradation is fully reversible by a short anneal in the dark [1,3], however, after the dissociation both the substitutional boron and the interstitial oxygen dimer are still present and the complex accordingly forms again under renewed illumination.

A way to permanently reverse the boron-oxygen related degradation has recently been proposed by Herguth et al. [4,5]. They reported on a nearly complete recovery of the open-circuit voltage of solar cells made on low-resistivity boron-doped Cz-Si by simultaneously illuminating and annealing the cells. In addition, a recovery of the bulk carrier lifetime was also demonstrated [4,5]. In a recently published study we were able to confirm these results qualitatively [6]. However, compared to the previously published results [4,5], higher temperatures were necessary in our experiments to completely deactivate the boron-oxygen complex.

In this work, we apply the regeneration procedure to RISE-EWT (Rear Interdigitated Single Evaporation Emitter Wrap-Through) solar cells [7] made on low-resistivity boron-doped Cz-Si which has an energy conversion efficiency of 19.1 % on an aperture area of 92 cm^2 after complete degradation. This value increases by more than 1 % absolute to 20.3 % and is shown to be stable under illumination at room temperature after applying our optimized deactivation process.

2 LIFETIME MEASUREMENTS

Lifetime experiments are performed on 1.4-Ωcm B-doped Cz-Si wafers with an interstitial oxygen concentration of $[O_i] = (7.5 \pm 0.5) \times 10^{17}$ cm^{-3}, as determined by Fourier-transform infrared spectroscopy. After an acidic damage etching and an RCA cleaning, a phosphorus diffusion is performed, resulting in an n^+-layer of ~100 Ω/sq on both sides of the wafers. This process is included because it accelerates the deactivation process by a factor of 3, as we have shown in a recent contribution [6,8]. Subsequently, the n^+-region is removed by a second acidic etching step after which the wafers are passivated by PECVD silicon nitride [9]. Lifetimes are measured at 300 K and a fixed injection level of $\Delta n = 10^{15}$ cm^{-3} using the quasi-steady-state photoconductance (QSSPC) technique [10].

In order to deactivate the boron-oxygen complex, we illuminate the lifetime samples on a hot-plate with a halogen lamp at light intensities between 70 and 100 mW/cm^2 . So far, results from two slightly different temperature ranges have been reported in the literature. Herguth et al. presented experiments performed at temperatures between 70 °C and 160 °C [4,5], whereas we found that higher temperatures between 140 °C and 215 °C are necessary [6]. The exact reason for this discrepancy is currently investigated in our lab.

The deactivation was shown to be thermally activated with an activation energy of 0.7 eV [4,5,6], resulting in a faster recovery of the carrier lifetime at higher temperatures. This acceleration of the deactivation, as well as the impact of the P-diffusion, is shown in Fig. 1. The open symbols correspond to P-diffused samples which were annealed at 165 °C (circles) and 198 °C (triangles), respectively, and illuminated at the same time at 0.7 suns (70 mW/cm^2). The increase in the deactivation speed with increasing temperature is clearly visible. At the same time, the deactivation rate of a P-diffused sample (open circles) is much higher than that of an as-grown sample (closed circle) at the same temperature.

The stability of the lifetime after the deactivation treatment under illumination at 1 sun is demonstrated in Fig. 2, which shows the evolution of the carrier lifetime in three different types of silicon samples with comparable resistivities (~ 1.4-Ωcm) and surfaces passivated by PECVD silicon nitride. The down triangles show that float-zone silicon (FZ-Si) with extremely low oxygen content suffers no lifetime degradation under illumination. In addition, this measurement verifies our

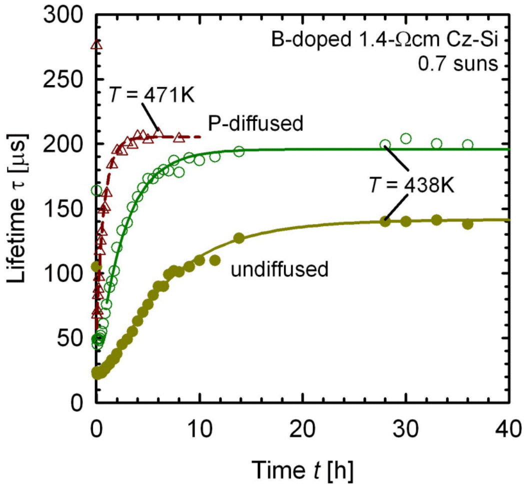

Figure 1: Time dependence of the lifetime τ of two P-diffused (open symbols) and one undiffused (closed circles) Cz-Si samples which are illuminated at 165 °C and 198 °C, respectively, at a light intensity of 70 mW/cm^2. The solid lines represent fits of an exponential rise to maximum function, which yield the time constants of the deactivation process.

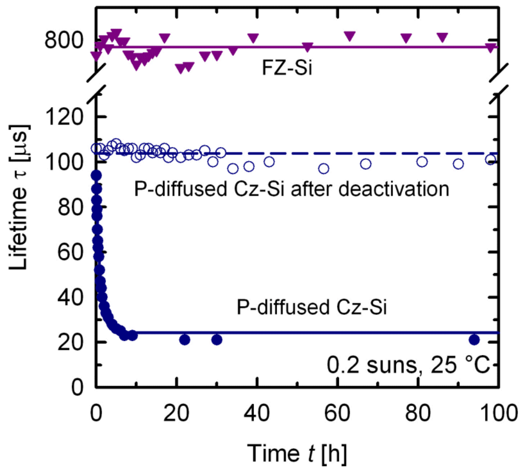

Figure 2: Comparison of the time dependence of the lifetime τ in oxygen-lean FZ-Si (down triangles), P-diffused Cz-Si (closed circles) and P-diffused Cz-Si which underwent the deactivation procedure (open circles).

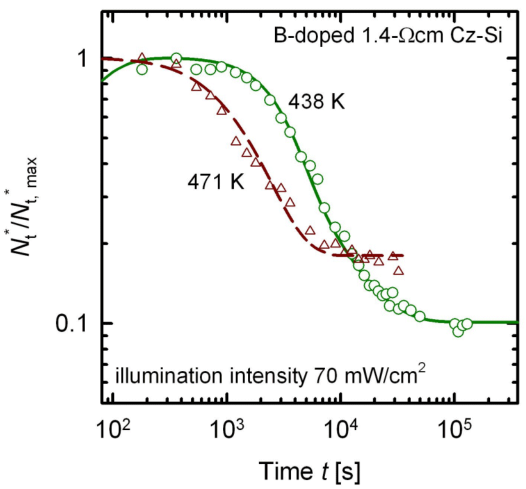

Figure 3: Measured (symbols) and calculated (lines) time dependence of the normalized defect concentration N_t^* obtained from the data of the P-diffused samples shown in Fig. 1 at two different temperatures (165 and 198 °C).

assumption that the silicon nitride surface passivation does not change during illumination. The filled circles in Fig. 2 show how the lifetime of an untreated P-diffused Cz-Si sample degrades within less than 10 h to a very low lifetime of only ~ 20 µs at an injection density of $\Delta n = 10^{15}$ cm^{-3}. By contrast, the lifetime of a comparable sample which underwent the deactivation treatment at 200 °C (open circles) is constant at 105 µs for more than 100 h.

3 THEORETICAL MODEL

Based on the experimental results we recently introduced a defect reaction model which is capable of explaining the complete time evolution of the carrier lifetime as shown in Fig. 1 [6]. As has been shown in previous publications [2,11], the initial lifetime degradation observed during the first few minutes of illumination can be explained by a recombination-enhanced defect reaction of a fast-diffusing oxygen dimer O_{2i} and an immobile substitutional boron atom B_s:

$$B_s + O_{2i} \rightleftharpoons B_sO_{2i}, \qquad (1a)$$

where the generation and dissociation rates of the B_sO_{2i} complex R_{a1} and R_{d1} have been experimentally determined with a high degree of accuracy [12]. In order to be able to model the lifetime recovery, a side defect reaction involving a complex XY of unknown composition was introduced. XY dissociates by a recombination-enhanced reaction into its components X and Y and one of the components, e.g. X, forms a complex XO_{2i} with the highly mobile oxygen dimer, leading to the reactions:

$$XY \rightleftharpoons X + Y \quad \text{and} \qquad (1b)$$

$$X + O_{2i} \rightleftharpoons XO_{2i}. \qquad (1c)$$

To experimentally verify this model, the time-dependent concentration of the B_sO_{2i} defect center deduced from the model has to be compared to experimental data, which in turn requires the solution of the corresponding rate equations. However, since the three reactions (1) all happen simultaneously, the rate equations of the seven involved compounds are interdependent. In order to simplify the problem, two assumptions are made:

(i) the concentration of substitutional boron $[B_s]$, which equals the doping concentration N_{dop}, is much larger than the concentration of oxygen dimers $[O_{2i}]$, and

(ii) the concentration of the species Y, i.e. [Y], is much larger than the concentration of the species X, i.e. [X].

Hence, $[B_s] = N_{dop}$ and [Y] can be assumed to be time-independent and two of the seven rate equations can

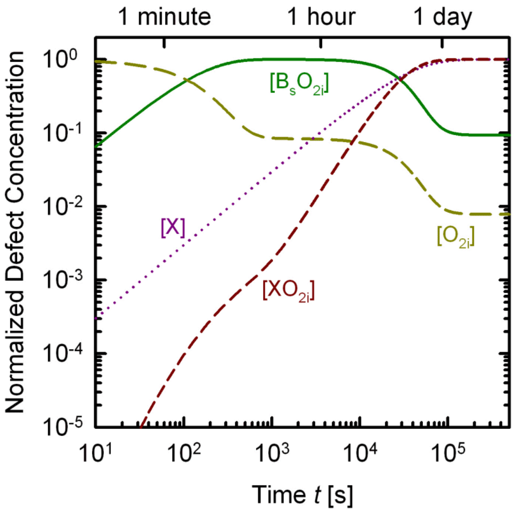

Figure 4: Simulated time dependence of the concentrations of the boron-oxygen complex (B_sO_{2i}), free oxygen-dimers (O_{2i}), the compound X and the recombination-inactive complex XO_{2i}. All concentrations are normalized to their maximum values.

be neglected. The five remaining rate equations are:

$$d[B_sO_{2i}]/dt = - k_{d1}\,[B_sO_{2i}] + k_{a1}\,[B_s]\,[O_{2i}], \tag{2a}$$

$$d[XY]/dt = - k_{d2}\,[XY] + k_{a2}\,[X]\,[Y], \tag{2b}$$

$$d[XO_{2i}]/dt = - k_{d3}\,[XO_{2i}] + k_{a3}\,[X]\,[O_{2i}], \tag{2c}$$

$$d[O_{2i}]/dt = k_{d1}\,[B_sO_{2i}] - k_{a1}\,[B_s]\,[O_{2i}] + k_{d3}\,[XO_{2i}] - k_{a3}\,[X]\,[O_{2i}], \tag{2d}$$

$$d[X]/dt = k_{d2}\,[XY] - k_{a2}\,[X]\,[Y] + k_{d3}\,[XO_{2i}] - k_{a3}\,[X]\,[O_{2i}], \tag{2e}$$

where k_{di} and k_{ai} are the dissociation and association rate constants, respectively. Note that $k_{d1} = R_{d1}$ and $k_{a1}N_{dop} = R_{a1}$ where R_{d1} and R_{a1} are the dissociation and association rates for the B_sO_{2i} complex reported in the literature [12]. Figure 3 depicts measured data (symbols) of the normalized defect concentration $N_t^* = 1/\tau(t) - 1/\tau_0$ divided by the maximum defect concentration $N_{t\ ,max}^*$, which was derived from the lifetime data shown in Fig. 1. In addition, Fig. 3 also shows theoretically calculated data (lines) for the normalized concentration of the boron-oxygen complex $[B_sO_{2i}]/[B_sO_{2i}]_{max}$. The calculation is done iteratively for all time-dependent concentrations in Eq. (2) by converting the differential equations into difference equations. As can be seen, an excellent agreement between theory and experiment is obtained.

An example of such an iterative calculation is shown in Fig. 4. At first, the concentration of the B_sO_{2i} complex increases, causing the concentration of oxygen dimers to decrease. After a few minutes, both the B_sO_{2i} and the O_{2i} concentration saturate, indicating that Eq. (2a) has reached quasi-equilibrium. Meanwhile, the complex XY slowly dissociates, resulting in an increase of the concentration of X. Once [X] has reached a critical level, free oxygen dimers and free X begin to form the complex XO_{2i}. At this point, boron-oxygen complexes begin to dissociate to retain the quasi-equilibrium of Eq. (2a) and the concentration of B_sO_{2i} accordingly decreases. This continues until the majority of oxygen dimers is bound in the complex XO_{2i}, at which point all four concentrations begin to saturate. In this calculation, which corresponds to the experimental data of the P-diffused sample treated at 135 °C, the final number of recombination-active boron-oxygen complexes was decreased by one order of magnitude.

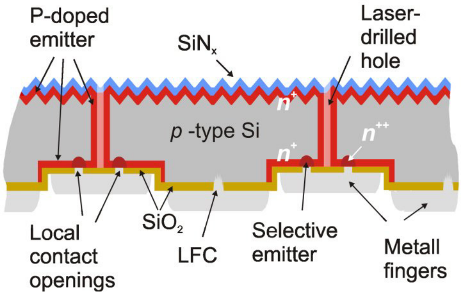

Figure 5: Schematic structure of a RISE-EWT solar cell [15].

4 APPLICATION OF THE DEACTIVATION PROCEDURE TO SOLAR CELLS

We have applied the deactivation procedure to high-efficiency RISE-EWT solar cells fabricated on low-resistivity B-doped Cz-Si. RISE-EWT solar cells were first introduced by Engelhart et al. [7]. A schematic of the RISE-EWT cell structure is shown in Fig. 5. Base and emitter fingers are interdigitated and on different height levels on the rear side of the cell. The n^+-emitter on the front is connected to the emitter on the back via laser-drilled holes (Emitter Wrap-Through structure [13]). The base region is contacted by laser-fired contacts (LFC) [14], which are formed through laser-firing of aluminium through a silicon-oxide layer. Fabrication steps include RCA cleaning, oxidation, front-surface texturing, laser structuring of the rear, laser drilling of holes, phosphorus diffusion, front-surface passivation, a single metallization step of the entire rear with self-aligning contact separation [7], and formation of the LFCs. Details of the solar cell process have been published elsewhere [15].

The base material of the cells investigated in this study is the same as that used in the lifetime measurements. Current-voltage characteristics were measured under standard testing conditions (25 °C, AM1.5G spectrum, 1 sun). The total cell area is 100 cm^2, however, due to a non-optimized busbar design the measurements presented here refer to an aperture area of 92 cm^2.

RISE-EWT solar cells made on FZ-Si have demonstrated energy conversion efficiencies of up to 21.4 % on an aperture area of 92 cm^2 [15]. On low-resistivity (1-2 Ωcm) boron-doped Cz-Si, we typically achieve efficiencies of (20.0±0.5) % before light-induced degradation and (19.0±0.5) % after complete degradation on the same illuminated cell area. Figure 6 shows the evolution of (a) the open-circuit voltage and (b) the efficiency of an exemplary RISE-EWT cell. The initial efficiency before light-induced degradation was 20.2 %.

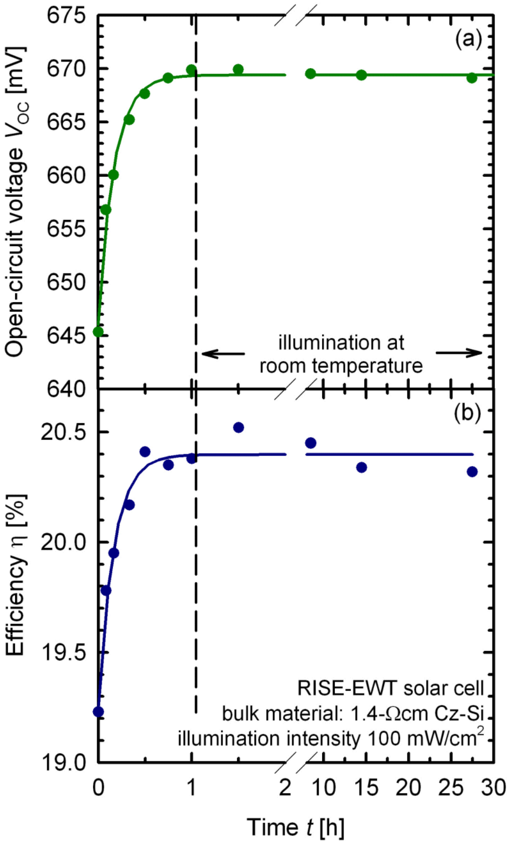

Figure 6: Time dependence of (a) the open-circuit voltage V_{OC}, and (b) the efficiency η of a high-efficiency RISE-EWT solar cell made on 1.4-Ωcm B-doped Cz-Si which is illuminated at 1 sun at 200 °C. After removal from the hot-plate, no efficiency degradation is discernible after several hours of illumination at room temperature.

After 8 h of illumination at room temperature using a halogen lamp at 0.2 suns, this value decreased to 19.2 %. The open-circuit voltage after degradation is 645 mV and the short-circuit current density 40.4 mA/cm^2. Note that the short-circuit current density shows only a negligible degradation because for EWT-type cells the short-circuit current density is less sensitive to reduced base diffusion lengths than for standard cells [16].

In order to deactivate the B_sO_{2i} complex the solar cell was illuminated at 200°C with a halogen lamp at a light intensity of 1 sun. As can be seen in Fig. 6, V_{OC} increases to nearly 670 mV after 60 min. J_{SC} remains the same within the uncertainty range (40.9 mA/cm^2), resulting in an energy conversion efficiency of 20.3 %. After more than twenty hours of illumination at room temperature the IV-characteristic was measured again, showing no significant loss of either V_{OC} or η. No further efficiency loss due to the formation of B_sO_{2i} complexes is thus expected. The time constant of the deactivation process determined from the measurements shown in Fig. 6 amounts to 9.98 min, which agrees well with the value of 9.02 min measured on lifetime samples under the same conditions.

5 CONCLUSIONS

In this work, we have shown that the light-induced degradation of the lifetime in B-doped Cz-Si due to the formation of the recombination-active boron-oxygen complex can be reversed through illumination at elevated temperature. The recovery of the lifetime has been modelled by introducing a second defect reaction in which the oxygen dimer is bound in a recombination-inactive complex. The numerical calculations derived from this model showed an excellent agreement with the experimental data. In addition, the deactivation procedure was applied to a high-efficiency RISE-EWT solar cell, resulting in a complete reversal of the light-induced degradation and a stable energy conversion efficiency of 20.3 %. To our knowledge this is the first solar cell on low-resistivity B-doped Cz-Si achieving a stabilized efficiency above 20 %.

ACKNOWLEDGEMENTS

Funding was provided by the State of Lower Saxony and the Federal Ministry for the Environment, Nature Conversation and Nuclear Safety (BMU) under contract number 0327650C. Parts of this work have been funded by Stiebel Eltron GmbH.

REFERENCES

[1] J. Schmidt, A.G. Aberle, and R. Hezel, Proc. 26th IEEE PVSC, Anaheim, CA (IEEE New York 1997), p. 13

[2] J. Schmidt and K. Bothe, *Phys. Rev. B* **69**, 024107 (2004)

[3] S.W. Glunz, S. Rein, W. Warta, J. Knobloch, and W. Wettling, Proc. 2nd WCPEC, Vienna, Austria, (Munich: WIP 1998), p. 1343

[4] A. Herguth, G. Schubert, M. Kaes, and G. Hahn, Proc. 21st EUPVSEC, Dresden, Germany, (Munich: WIP 2006), p.530

[5] A. Herguth, G. Schubert, M. Kaes, and G. Hahn, *Prog. Photovolt: Res. Appl.* **16**, 135 (2008)

[6] B. Lim, K. Bothe, and J. Schmidt, *phys. stat. sol. (RRL)* **2**, 93 (2008)

[7] P. Engelhart, A. Teppe, A. Merkle, R. Grischke, R. Meyer, N.-P. Harder, and R. Brendel, Technical Digest 15th PVSEC, Shanghai, 2005, p. 802

[8] B. Lim, K. Bothe, and J. Schmidt, Proc. 33rd IEEE PVSC, San Diego, 2008

[9] T. Lauinger, J. Schmidt, A.G. Aberle, and R. Hezel, *Appl. Phys. Lett.* **68**, 1232 (1996)

[10] R. Sinton and A. Cuevas, *Appl. Phys. Lett.* **69**, 2510 (1996)

[11] D. Palmer, K. Bothe, and J. Schmidt, *Phys. Rev. B* **76**, 035210 (2007)

[12] K. Bothe and J. Schmidt, *J. Appl. Phys.* **99**, 013701 (2006)

[13] J.M. Gee, W.K. Schubert, and P.A. Basore, Proc. 23rd IEEE PVSC, Lousville, 1993, p. 265

[14] E. Schneiderlöchner, R. Preu, R. Lüdemann, S.W. Glunz, and G. Willeke, Proc. 17th EC-PVSEC, 2001, p. 1303

[15] S. Hermann, P. Engelhart, A. Merkle, T. Neubert, T. Brendemühl, R. Meyer, N.-P. Harder, and R. Brendel, Proc. 22nd EUPVSEC, Milan, Italy (Munich: WIP 2007), p. 970

[16] J. Dicker, J. Sölter, J.O. Schumacher, S.W. Glunz, and W. Warta, Proc. 28th IEEE PVSC, Anchorage, 2000, p. 387